Voltage Control of Perpendicular Magnetic Anisotropy in Multiferroic $(Co/Pt)_3/PbMg_{1/3}Nb_{2/3}O_3$-$PbTiO_3$ Heterostructures

Qu Yang,[1] Tianxiang Nan,[2] Yijun Zhang,[1] Ziyao Zhou,[1] Bin Peng,[1] Wei Ren,[1,3] Zuo-Guang Ye,[1,3,4] Nian X. Sun,[1,2] and Ming Liu[1,3,*]

[1]*Electronic Materials Research Laboratory, Key Laboratory of the Ministry of Education & International Center for Dielectric Research, Xi'an Jiaotong University, Xi'an 710049, People's Republic of China*

[2]*Department of Electrical and Computer Engineering, Northeastern University, 360 Huntington Avenue, Boston, Massachusetts 02115, USA*

[3]*Collaborative Innovation Center of High-End Manufacturing Equipment, Xi'an Jiaotong University, Xi'an 710049, People's Republic of China*

[4]*Department of Chemistry and 4D LABS, Simon Fraser University, Burnaby, British Columbia V5A 1S6, Canada*

(Received 11 May 2017; revised manuscript received 29 August 2017; published 16 October 2017)

Voltage control of perpendicular magnetic anisotropy (PMA) is very promising in the realization of high-density, lightweight, and energy-efficient information storage. However, it is hard to achieve *E*-field regulation of PMA in conventional multiferroic laminates since the voltage-induced magnetic anisotropy is relatively small. In this study, we demonstrate *E*-field control of PMA in $(Co/Pt)_3/Pb(Mg_{1/3}Nb_{2/3})O_3$-$PbTiO_3$ multiferroic heterostructures at room temperature using ferromagnetic resonance measurement (FMR) and a magnetic optical Kerr (MOKE) microscope. When a single Co layer (t_{Co}) = 1.0 nm PMA is obtained, a resonance shift up to 470 Oe is obtained with a 12-kV cm^{-1} *E* field. Up to 75% perpendicular magnetic moments can be controlled with an applied 10-kV cm^{-1} electric field at $t_{Co} = 0.9$ nm while little effect is obtained at $t_{Co} = 0.7$ nm. In addition, a multiferroic heterostructure with in-plane anisotropy is also studied at $t_{Co} = 1.4$ nm, and the resonance shifts are comparable to 1.0 nm. We relate this phenomenon to the instability of Co orbital moments near the critical transition area (0.9, 1.0, 1.4 nm). However, if t_{Co} is far from the transition point, the magnetic properties become insensitive to an external stimulus (0.7 nm). This voltage manipulation of PMA in ultrathin Co films should offer possibilities for realizing electronic devices and memories with great energy efficiency.

DOI: 10.1103/PhysRevApplied.8.044006

I. INTRODUCTION

Co-based materials have drawn much attention in magnetic recording since they offer an approach to solving the limitations associated with superparamagnetic grains [1,2]. Based on perpendicular magnetic anisotropy (PMA), these systems show a promising way to enable high-performance spintronic and logic devices for their ability to enhance thermal stability and ultrahigh storage density [3–6]. Spin reorientation transition (SRT) offers a typical way to achieve PMA at room temperature [6–8]. Based on ultrathin ferromagnetic films, the magnetic easy axis can be rotated from the in-plane to out-of-plane direction as the film thickness or temperature decreases [8–10]. For Co/Pt multilayers, the Co 3*d*–Pt 5*d* hybridization localized at the interface can give rise to a strong perpendicular orbital moment [11,12]. As the thickness of a single Co layer (t_{Co}) decreases, the interface effect gradually overcomes the volume effect and enhances the PMA [11].

To utilize the PMA in further miniaturized spintronic devices, one major concern is to find an energy-efficient way to manipulate it [13]. Earlier studies have proven that strain is effective in controlling this interfacial PMA [12,14]. Meanwhile, the voltage-induced strain effect on magnetic anisotropy has been widely studied over the past decade in multiferroic heterostructures [15–22], which is very promising in nonvolatile, lightweight, and energy-efficient magnetic memories [23–25]. Therefore, it will be very interesting to combine PMA and multiferroics to study *E*-field control of PMA. However, in conventional multiferroic laminates, it is hard to achieve the *E*-field regulation of PMA for the relatively small voltage-induced magnetic anisotropy [18]. Therefore, the study of magnetization switching is mostly limited in the film plane [26–28]. Although there are some previous studies that investigated strain-induced changes in PMA via hysteresis loops [29–31] or domain-wall motion [5], the quantitative explorations of magnetic anisotropy under room temperature are

*To whom all correspondence should be addressed. mingliu@xjtu.edu.cn

still at a premium. Although there were two related works recently [32,33] on how the interface effect enhances the magnetostriction of ultrathin Co films and how this effect leads to a considerable PMA regulation, the results are still rarely reported [32,34].

In this work, we obtain Co/Pt multilayers with PMA and in-plane anisotropy on $Pb(Mg_{1/3}Nb_{2/3})O_3$-$PbTiO_3$ (PMN-PT)(001) substrates through thickness-driven SRT. Having a large d_{33} piezoelectric coefficient (approximately 2000 pC/N) [35], (001)-oriented PMN-PT is suitable for the voltage control of the perpendicular direction. In addition, it can generate a sizeable lattice distortion along the diagonal axes (i.e., the [110] direction) through 109° ferroelectric domain switching, also making itself outstanding in the in-plane direction [16,36]. Ferromagnetic resonance (FMR) measurements are mainly utilized to study voltage-controlled PMA and the strain-mediated magnetoelectric (ME) coupling at room temperature. A 470-Oe FMR upward shift of a perpendicular 1.0-nm $(Co/Pt)_3$ film is observed with an applied $E = 12\ \mathrm{kV\,cm^{-1}}$. Repeatable dynamic switching of PMA at room temperature is demonstrated, which is favored for its low energy consumption. In addition, voltage control of perpendicular domain switching is achieved through a room-temperature magnetic optical Kerr (MOKE) microscope, which is favored for its high sensitivity [37] and can maintain a high-quality signal even if the Co layer is extremely thin. Based on 0.9-nm $(Co/Pt)_3$, up to 75% magnetic moments can reverse under 10 $\mathrm{kV\,cm^{-1}}$, while little effect is observed in a 0.7-nm multilayer. In addition, the ME coupling behavior is also observed when $t_{Co} = 1.4$ nm, which is a little bit thicker than the transition point (1.2 nm). Considerable resonance shifts of 1.4 nm are obtained in both the in-plane and out-of-plane directions. We relate the differences in the voltage-control effect to the stability of Co orbital moments. Near the transition area (0.9, 1, 1.4 nm), perpendicular and in-plane Co orbital moments are unstable [11], which can respond to voltage easily, leading to effective regulations. However, when the thickness is a little bit far from the transition area, the Co orbital moments become unchangeable and insensitive to an external stimulus like voltage [33]. Our work provides a promising platform for the realization of energy-efficient spintronic memories.

II. EXPERIMENT

A. Sample preparation

Multilayers with a structure of Ta(2 nm)/$[Co(t_{Co})/Pt(1\ nm)]_3$/Pt(1 nm)/Ta(3 nm) are deposited onto a PMN-PT(001) single crystal ($4 \times 5 \times 0.5\mathrm{mm^3}$) by dc magnetron sputtering at room temperature. The base pressure is 1.5×10^{-7} Torr and increases to 3 mTorr during the evaporation. The working dc power is 20–30 W. A Pt layer with a thickness of 10 nm is sputtered on the bottom of the PMN-PT as an electrode.

B. Experimental characterization

In situ voltage control is carried out with a MOKE microscope (Evico Magnetics, em-Kerr-Highres) and FMR (JEOL, JES-FA200) measurements. FMR is carried out with a microwave cavity operating at TE 011 mode at 9.2 GHz. For the domain observation carried out by the MOKE microscope, we use the polar MOKE mode with a perpendicular electromagnet. We use a Keithley 6517B electrometer for the applied voltage. All the characterizations are performed at room temperature.

III. RESULTS AND DISCUSSION

In order to study the voltage control of PMA, we fabricate Ta/$[Co(t_{Co})/Pt]_3$/Pt/Ta/PMN-PT(001) multiferroic heterostructures by magnetron sputtering at room temperature. The magnetic easy axis can be regulated with variation of t_{Co} (i.e., thickness-driven SRT). When t_{Co} decreases to 1.0 nm, PMA can be characterized clearly via magnetic force microscope (MFM), MOKE, and FMR. Figure 1(a) shows a MFM image for this 1.0-nm sample. Two different randomly oriented domains are observed without exposing the sample to magnetic field. This domain structure is caused by the dipolar interaction related to spin orientation, which is an intrinsic property of the film without relevance to the surface morphology [38].

The magnetization state can be precisely controlled with thickness variation in our multiferroic heterostructures. Figure 1(b) shows the hysteresis loops measured with polar MOKE for the samples with PMA. When $t_{Co} \leq 1.0$ nm, all three ultrathin films ($t_{Co} = 0.6$, 0.8, and 1.0 nm) possess square shapes with a typical perpendicular easy axis. The 1.0-nm Co layer occupies the smallest coercive field, corresponding to the lowest energy barrier and highest energy utilization. In order to figure out the details of the anisotropies and determine the *E*-field regulation of PMA precisely, FMR is utilized. It is carried out in a resonant cavity and measured by the rotation of the external magnetic field along the normal plane. In this work, 0° represents the *H* field applied along the in-plane direction, while 90° is the out-of-plane direction. A larger resonance field indicates that higher magnetic energy is needed during the uniform precession process, corresponding to the hard magnetization direction. The measurement configuration can be seen in Fig. 1(c), where the sample is placed parallel to the *x*-*z* plane, while the electric field (*E* field) is applied across the PMN-PT substrate.

Figure 1(d) is the angular dependence of the FMR field, and the results indicate the existence of a transition point of t_{Co} which determines the occurrence of PMA. It can be seen that the magnetic easy axis transforms from in plane to out of plane (i.e., PMA) when t_{Co} decreases from 1.4 nm (red open circles) to 1.0 nm (blue open squares), and the transition point turns out to be around 1.2 nm (black open hexagon). Moreover, we can calculate the anisotropy field

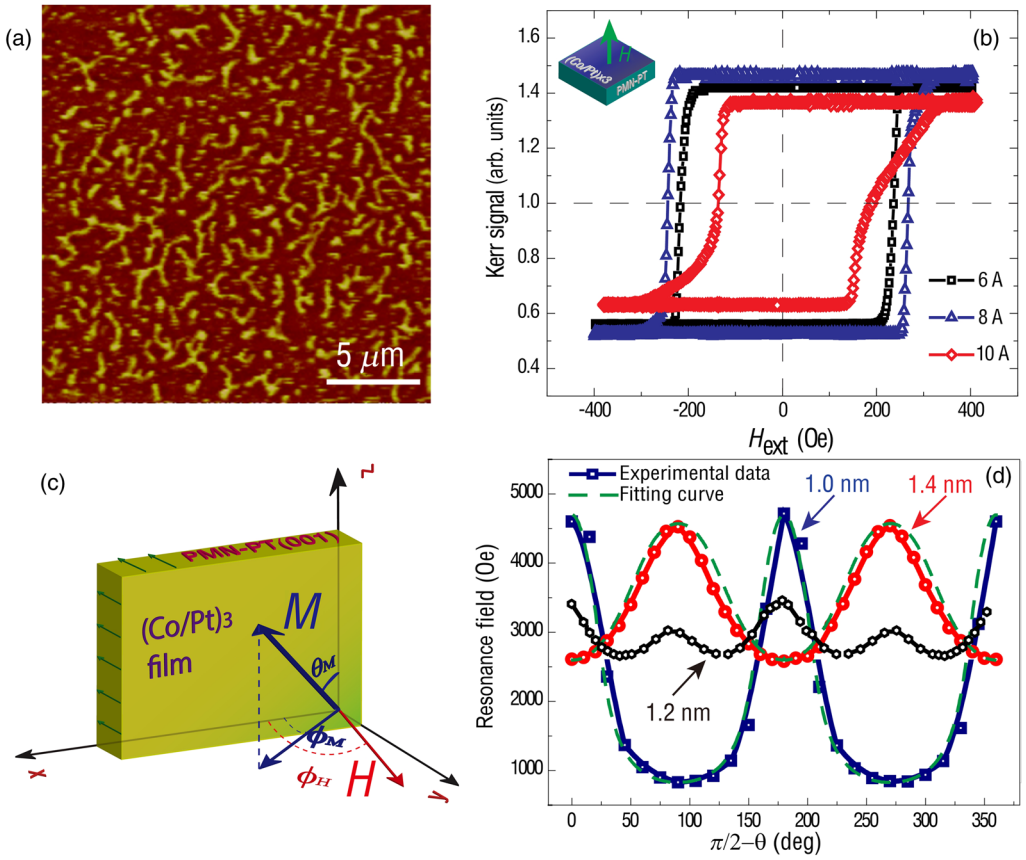

FIG. 1. (a) MFM image of 1.0-nm $(Co/Pt)_3$ film on PMN-PT(001) substrate, showing a ferromagnetic multidomain. (b) Out-of-plane magnetic hysteresis loops of $(Co/Pt)_3$/PMN-PT(001) plotted against Co thickness. (c) Schematic of the measurement configuration for the $(Co/Pt)_3$/PMN-PT(001) heterostructures. The definition of the angles is the same with respect to the measurement and fitting progress. (d) Angle dependence of the FMR field. Measured curves for Co thickness of $t = 1.0$ (blue open squares), 1.2 nm (black open hexagon), and 1.4 nm (red open circles) at room temperature compared with simulated results (green dashed line).

according to the measured resonance field based on Eq. (1) proposed by Chappert *et al.* [39]

$$\left[\frac{\omega}{\gamma}\right]^2 = [H\cos(\varphi_H-\varphi_M)+(4\pi M-H_{A1}-H_{A2})\cos 2\varphi_M + H_{A2}(3\sin^2\varphi_M\cos^2\varphi_M-\sin^4\varphi_M)] \times [H\cos(\varphi_H-\varphi_M) -(4\pi M-H_{A1}-H_{A2})\sin^2\varphi_M-H_{A2}\sin^4\varphi_M], \quad (1)$$

where ω is the angular resonance frequency (9.2 GHz $\times 2\pi$), γ is the gyromagnetic ratio of 2.8 MHz/Oe, H is the resonance field, and 4πM is 17.7 kOe at room temperature. H_{A1} and H_{A2} correspond to the first and second anisotropy energy terms. Based on this equation, the calculated anisotropy field can further derive the theoretical resonance field as shown by green dashed lines in Fig. 1(d). When it comes to the critical thickness of SRT, higher orders of energy terms should be involved to guarantee an accurate theoretical analysis, which is demonstrated in our previous work [10].

It is worth mentioning that the first- and second-order energy terms, which can be expressed by $K_i = K_i^V + 2K_i^S/t_{Co}$ ($H_{A1} = 2K_1/M$, $H_{A2} = 4K_2/M$), are determined with consideration of both the volume contribution K_v and the surface contribution K_s [10,39]. Polycrystal grown by dc rf magnetron sputtering [40] and pulsed laser deposition [41–43] is often reported to show a preferred orientation of the crystallographic [111] axis oriented parallel to the substrate normal. We consider our Co/Pt multilayers to be mostly (111) textured ferromagnetic (FM) grains. As revealed by Liu *et al.* [41], in (111) textured FM films, the magneto-texture anisotropy energy of the bulk contribution is only about 2% of the surface contribution when the film thickness is 10 nm. Therefore, in our Co/Pt(111) multilayers with a much thinner film thickness of 0.6–1.4 nm, we believe that the volume effect is negligible, and the interface anisotropy dominates in the first- and second-order energy terms.

The room-temperature magnetization control of PMA with E field is first examined in $t_{Co} = 1.0$ nm $(Co/Pt)_3$/PMN-PT(001) multiferroic heterostructures. As shown in Fig. 2(a), the resonance field out of plane keeps increasing as the E field goes close to the saturation point (10 kV cm^{-1}). Eventually, a maximum resonance field shift of 470 Oe can be observed at the saturation voltage. To further confirm the E-field effect on FMR, the angle dependence of the FMR field is carried out at 0 and 10 kV cm^{-1}. As shown in Fig. 2(b), the electrically controllable FMR fields at different angles maintain robust and stable shifts. The external E field gives rise to a strain on the piezoelectric phase of the PMN-PT substrate, leading to a stress on the overlayer's magnetic phase through ME coupling. Given that the $(Co/Pt)_3$ film occupies an ultrathin

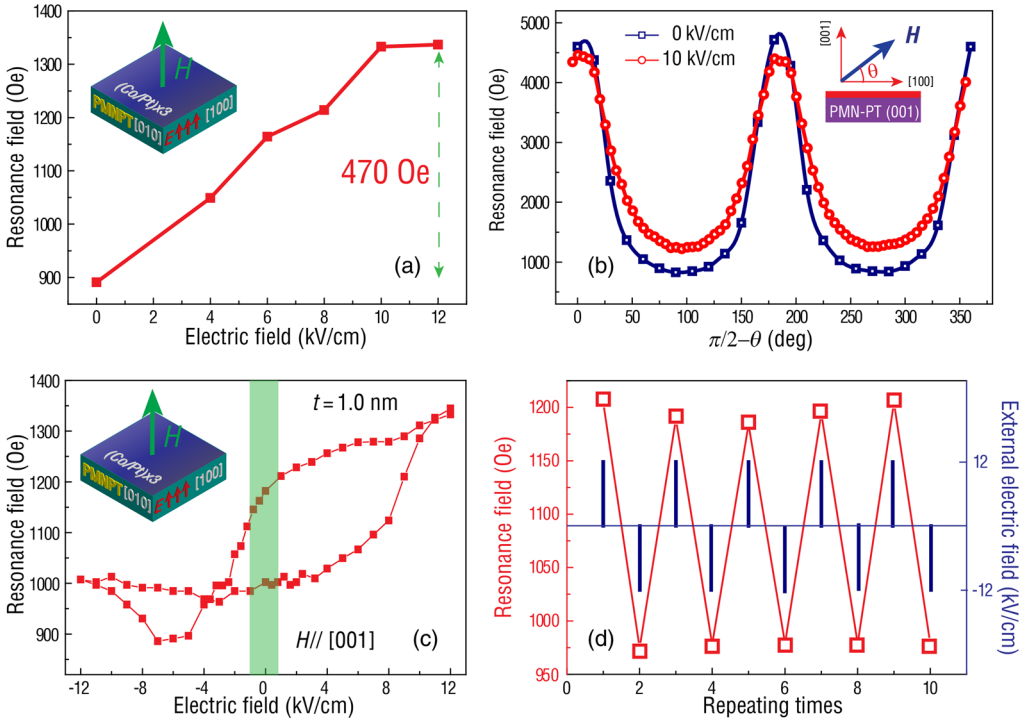

FIG. 2. *E*-field tuning of 1.0-nm $(Co/Pt)_3$/PMN-PT(001) in the out-of-plane direction. (a) Resonance field for the out-of-plane direction. (b) Angular dependence of the FMR field with and without the external *E* field applied along the PMN-PT substrate. (c) Butterfly curve of *E* fields between −12 and +12 kV cm^{-1}. (d) FMR field switching during repeated ±12-kV cm^{-1} voltage pulse, corresponding to the green banded rectangular region of (c).

thickness compared to that of the PMN-PT(001) substrate, the film should undergo the same strain states as the PMN-PT(001), thus, enabling the *E*-field control of the FMR field by strain-mediated coupling [23,26]. We confirm this theory below [Fig. 2(c) and Figs. 4(a) and 4(c)], and it acts as the basis for the following discussion on the "butterfly" curve as well as the reserved *E*-field manipulation of magnetism in $(Co/Pt)_3$/PMN-PT(001) heterostructures.

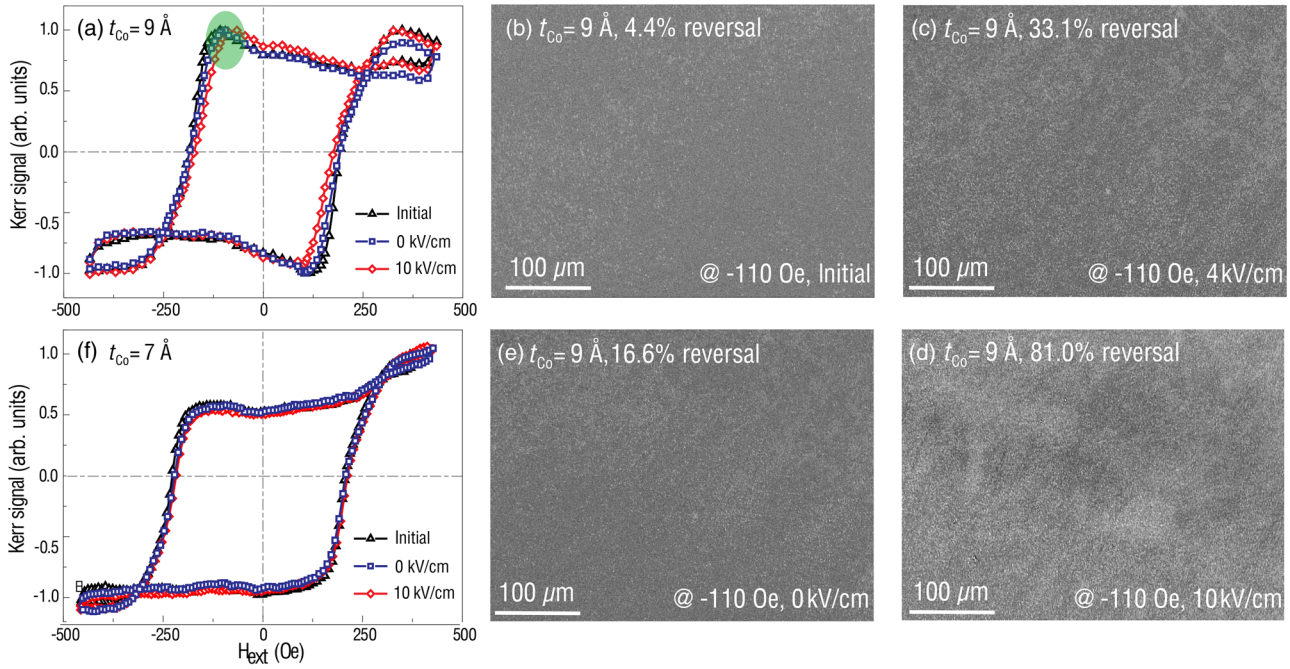

FIG. 3. *In situ* voltage control of hysteresis loops and domain switching in $(Co/Pt)_3$/PMN-PT(001) heterostructures evidenced by the polar MOKE mode. (a) *E*-field control of hysteresis loops at $t_{Co} = 0.9$ nm. (b)–(e) are corresponding domain nucleations. Clear domain-switching enhancements can be obtained while under external applied voltage. The determination of the reversal ratio: count the ratio of light first and then normalize by the value of the saturated image. (f) *E*-field control of hysteresis loops at $t_{Co} = 0.7$ nm, confirming that there is no obvious tuning effect when PMA is too strong.

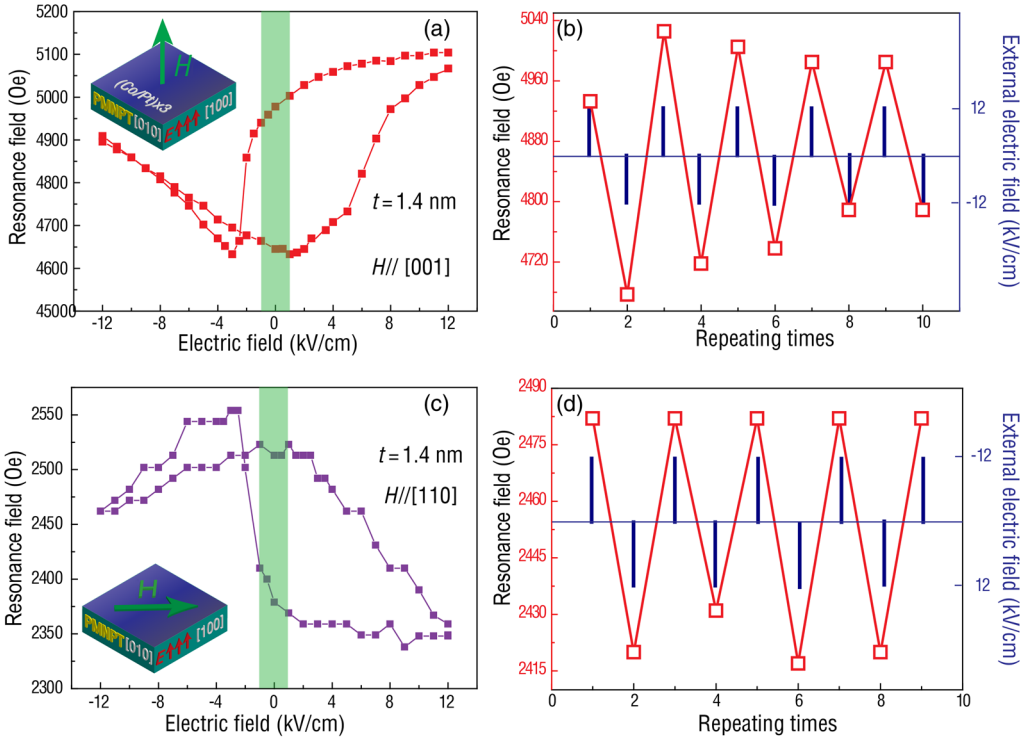

FIG. 4. Butterfly curves and FMR field switches out of plane (a),(b) and in plane (c),(d) based on 1.4-nm $(Co/Pt)_3$/PMN-PT(001).

In Fig. 2(b), it is obvious that the applied E field reduces the differences between in plane and out of plane, which means that PMA is weakened. The influence of the biaxial strain on the interface anisotropy can be quantitatively studied based on the Kittel equation according to a simplified phenomenological model [15]:

$$\frac{\omega}{\gamma} = H + H_k + H_{\text{eff}} - 4\pi M, \tag{2}$$

where H_k relates to the volume magnetocrystalline anisotropy, and H_{eff} refers to the E-field-induced effective magnetic field, which is influenced by the change of the interface anisotropy. In our heterostructure, the magnetostrictive coefficient of Co $(\lambda_s) \sim -62 \times 10^{-6}$ and H_{eff} is found to be in proportion to $\lambda_s \sigma_E / M_s$ [15]. σ_E refers to the voltage-induced stress. Since the piezoelectric coefficient of PMN-PT(001) is positive ($d_{33} \sim 2000$ pC/N) [35], σ_E represents tensile stress along the [001] direction. This 470-Oe out-of-plane FMR field upward shift is a result of negative H_{eff} in Eq. (2), which leads to increasing H_r because the other factors almost keep constant.

However, typical stress-induced anisotropy is quite limited without the consideration of the interface. As demonstrated by Peng *et al.* [32], no more than a 160-Oe resonance shift can be obtained even though the applied E field is as large as 12 kV cm^{-1}. Therefore, the pure strain effect cannot explain this 470-Oe resonance field shift. In addition, the buffer Ta layer (3 nm) and bottom Pt layer (1 nm) manage to avoid charge accumulation at the interface of Co and PMN-PT, thus, excluding the charge effect during this voltage-control process [32,44,45].

It has been demonstrated that the origin of the perpendicular orbital moment is strongly related to the Co $3d$–Pt $5d$ interfacial hybridization [11]. The tensile strain along the z direction will increase the distance between Co and Pt, which leads to a strain-induced suppression of the interfacial hybridization [32,33]. Such a reduction of Co $3d$–Pt $5d$ hybridization gives an explanation for the observed weaker PMA.

Meanwhile, repeatable switching of PMA is also studied since it is important for memory properties [46]. In this manipulation, the magnetism is controlled by voltage impulse instead of voltage bias [26]. Here, we demonstrate repeatable magnetization switching in $t_{\text{Co}} = 1.0$ nm $(Co/Pt)_3$/PMN-PT with external E fields between -12 and $+12$ kV cm^{-1}. As shown in Fig. 2(c), when the E field switches back to 0 kV cm^{-1} from positive to negative or vice versa, two different FMR fields come out, as displayed in the green rectangular region. The two distinct remnant states indicate the realization of repeatable magnetism modulation. The resonance field versus the repeating number of E-field square pulses (blue vertical line) is further studied to test the stability of these two states [Fig. 2(d)]. The difference in the FMR field between the $+12$- and -12-kV cm^{-1} voltage pulse can be observed clearly and stably, confirming good repeatability.

When t_{Co} is less than 1 nm, it is difficult for the FMR study because of the extremely weak signal. Therefore, we utilize *in situ* Kerr microscopy to study the voltage control of PMA for the $(Co/Pt)_3$/PMN-PT(001) multilayers at $t_{\text{Co}} =$ 0.9 nm and $t_{\text{Co}} = 0.7$ nm. Figure 3 shows the evolutions of the hysteresis loops and perpendicular domains during the

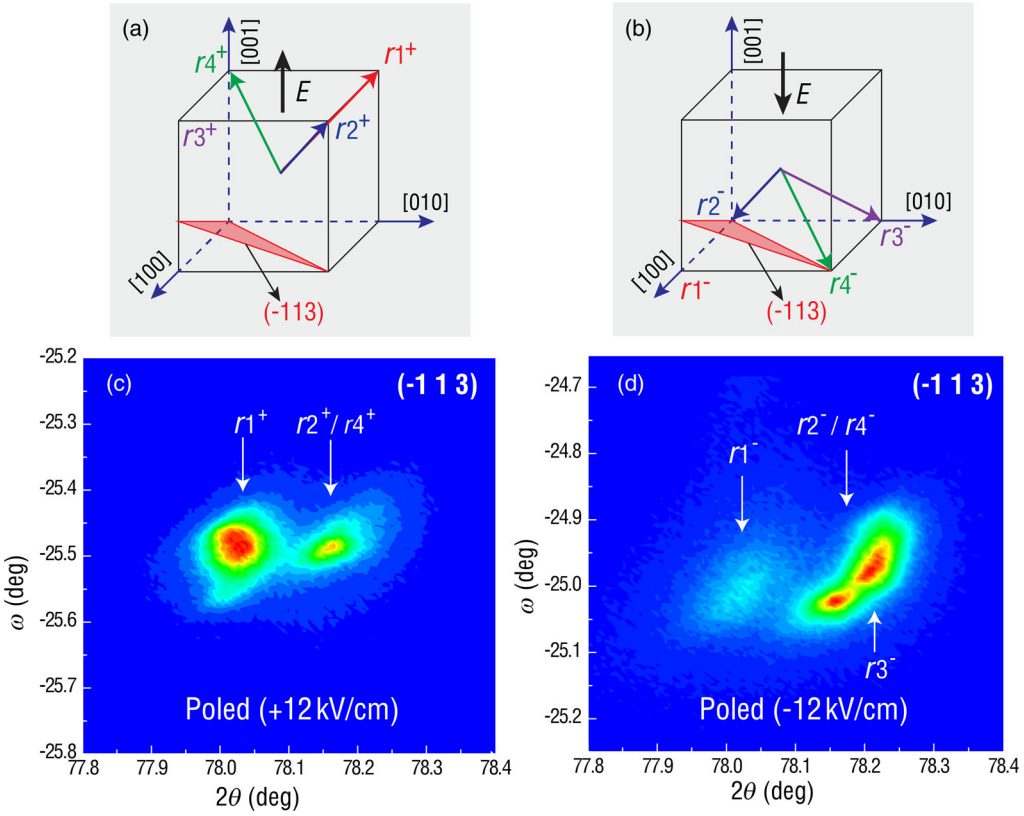

FIG. 5. Schematics of domain structures for PMN-PT(001) substrate after $+12\text{-kV cm}^{-1}$ (a) and -12-kV cm^{-1} (b) polarization. (c),(d) are the corresponding RSM images in the vicinity of the (−113) reflections, respectively, and are measured based on two different PMN-PT(001) substrates. The sample for (c) is polarized by $+12\ \text{kV cm}^{-1}$, and the sample for (d) is first polarized by $+12\ \text{kV cm}^{-1}$ and then switched to $-12\ \text{kV cm}^{-1}$.

control process. Figures 3(a)–3(e) are the results at $t_{\text{Co}} = 0.9$ nm. The out-of-plane hysteresis loops in Fig. 3(a) serve as a reference for the perpendicular magnetic moment switching, and we find that the out-of-plane direction becomes harder while under external voltage. Figures 3(b)–3(e) are the corresponding domain images. At each applied voltage, we saturate the samples with a large positive H field (+1000 Oe) and then decrease the H field until it reaches the same negative spin-flip field (−110 Oe), where domain switching starts to be active, to observe the domain-reversal ratio. As shown in Fig. 3(b), at the initial state, only 4.4% of the domain reverses. When the applied E field gradually increases to 4 kV/cm, the reversal ratio goes up to 33.1% [Fig. 3(c)]. We then make the E field 10 kV/cm, and the ratio rises to 81% [Fig. 3(d)], indicating that up to 75% of perpendicular magnetic moments can be controlled with the applied voltage. In addition, most of the moments turn back when the voltage is switched off [Fig. 3(e)], confirming good reversibility.

It has been proven that magnetic properties become insensitive to an external stimulus like voltage [33] and temperature variation [10] when the Co layer is too thin or too thick from the transition point. Figure 3(f) is the result for $t_{\text{Co}} = 0.7$ nm, which has a strong PMA. In this case, the applied voltage can hardly influence the magnetic moments. This is probably because the perpendicular Co orbital moments in the Co 3*d*–Pt 5*d* hybridization [11] are too stable to be affected by the external stimulus.

Another strain-mediated electric field modulation of magnetism is also studied here in $t_{\text{Co}} = 1.4$ nm $(\text{Co/Pt})_3$/PMN-PT with in-plane anisotropy (near the transition point). For the (001)-oriented ferroelectric substrates, 109° ferroelastic switching produces in-plane lattice distortions along the diagonal axes ([110] direction) [16,36] and thereby contributes to a distinct ME coupling (as we demonstrate in Fig. 5). For the out-of-plane direction [[001], Fig. 4(a)], a maximum upward shift of up to 566 Oe is obtained, and the maximum resonance shift for the in-plane direction [[110], Fig. 4(b)] is 216 Oe. The 1.4-nm sample with in-plane anisotropy and the mentioned 1.0-nm sample with PMA have the same response order of magnitude, probably because they are both near the transition area (1.2 nm), and the in-plane and perpendicular Co orbital moments [11] are unstable, so an external stimulus like voltage can influence their magnetic properties. In addition, we also demonstrate the repeatability of the voltage-control effect for this 1.4-nm $(\text{Co/Pt})_3$/PMN-PT heterostructure in both directions [Figs. 4(b) and 4(d)], which paves a fascinating way for the development of magnetoelectric random access memories (MERAMs).

High-resolution x-ray-diffraction measurements are also carried out to figure out the polarization-switching pathway of PMN-PT during E-field modulation. Reciprocal-space mapping (RSM) images for rhombohedral PMN-PT(001) single crystals are displayed in Fig. 5. $r1$, $r2$, $r3$, and $r4$ along body diagonals represent four ferroelectric domains

of the pseudocubic unit cell, while the "+" and "−" signs represent the "up" and "down" polarization directions, respectively. When a vertical voltage is applied and removed, there are three possible ferroelastic switching pathways: (1) 71° polarization switching from $r1^+$ to $r3^-$ (or $r4^+$), (2) 109° polarization switching from $r1^+$ to $r3^+$ (or $r4^-$), and (3) 180° polarization switching from $r1^+$ to $r1^-$. According to the spot distribution of (−113) planes, these four structural domains ($r1$–$r4$) can be distinguished. As $+12$ kV cm^{-1} is vertically applied and then switched off, the RSM image in Fig. 5(c) shows that about 70% of polarizations stay as the $r1$ domain and $r2/r4$ acquires a relatively low intensive spot. The absence of the $r3$ domain structure may be attributed to a slight miscut of the PMN-PT substrate, which can be evidenced by the spot intensity distribution in the RSM patterns [16]. Upon poling the sample with a negative field of -12 kV cm^{-1}, the polarization flips from the upward to the downward direction. As shown in Fig. 5(d), a highly weaker $r1$ polarization is observed, and an additional high-intensity reflection spot appears, corresponding to the $r3$ domain state. This polarization switching indicates that 71° ($r1^+$ to $r3^-$), 109° ($r1^+$ to $r4^-/r2^-$, $r2^+/r4^+$ to $r3^-$) and 180° ($r1^+$ to $r1^-$) polarization switching all take place during this progress and, thus, generates a new domain structure with large lattice strain. During the polarization reversal, only the 109° ferroelastic switching produces lattice strains in the (001) plane along the two diagonal axes and thereby contributes to a sizable ME coupling [16]. Eventually, a stable and repeatable polarization rotation with distinct ferroelectric domain switching is confirmed for the reserved and reversible FMR field modulation achieved in Figs. 3 and 4.

Nevertheless, the origin of the significant ME coupling during this electric-field-assisted magnetization manipulation is not a result of the pure strain effect. As demonstrated in the previous work, the effective regulation should be based on an interfacial elastic strain [14,47], which is reflected by t_{Co} (0.9, 1.0, and 1.4 nm) near the transition point in our case. At the critical transition area, the in-plane and perpendicular Co orbital moments are unstable, making the samples sensitive to the strain-mediated voltage tuning. That probably explains the observed 75% domain reversal and giant (470–566)-Oe resonance shift in the out-of-plane direction.

IV. CONCLUSION

In summary, we demonstrate an E-field-assisted manipulation of magnetization based on $(Co/Pt)_3$/PMN-PT(001) multiferroic heterostructures with t_{Co} near the magnetic easy-axis transition area. Through FMR measurement, both an electric dependent butterfly curve and repeatable switching are observed at room temperature for the heterostructures with and without PMA. Attributed to the unstable Co orbital moments in the critical transition area, up to 470- and 566-Oe voltage-induced resonance shifts are realized in both samples. In addition, voltage control of perpendicular domain switching is demonstrated which proves to be effective in the regulation of dynamic magnetization reversal. This ferroelastic switching of magnetic anisotropy is important in the realization of electronic devices and memories.

ACKNOWLEDGMENTS

This work is supported by the Natural Science Foundation of China (Grants No. 51472199, No. 11534015, and No. 51602244), the Natural Science Foundation of Shaanxi Province (Grant No. 2015JM5196), the National 111 Project of China (Grant No. B14040), the 973 Program (Grant No. 2015CB057402), and the Fundamental Research Funds for the Central Universities. B. P. acknowledges support from the China Postdoctoral Science Foundation (Grant No. 2016M590939). Z.-G. Y. acknowledges support from the Natural Sciences and Engineering Research Council of Canada (Grant No. 203773). Z. Z. and M. L. are supported by the China Recruitment Program of Global Youth Experts.

We thank Jie Hu for his contribution to this work.

[1] G. J. Kusinski, K. M. Krishnan, G. Thomas, and E. Nelson, Domain structures and temperature-dependent spin reorientation transitions in c-axis oriented Co-Cr thin films, J. Appl. Phys. **87**, 6376 (2000).

[2] G. J. Kusinski, K. M. Krishnan, G. Denbeaux, and G. Thomas, Magnetic reversal of ion beam patterned Co/Pt multilayers, Scr. Mater. **48**, 949 (2003).

[3] D. Chiba, M. Kawaguchi, S. Fukami, N. Ishiwata, K. Shimamura, K. Kobayashi, and T. Ono, Electric-field control of magnetic domain-wall velocity in ultrathin cobalt with perpendicular magnetization, Nat. Commun. **3**, 888 (2012).

[4] M. Farle, W. Platow, A. Anisimov, P. Poulopoulos, and K. Baberschke, Anomalous reorientation phase transition of the magnetization in fct Ni/Cu(001), Phys. Rev. B **56**, 5100 (1997).

[5] P. Shepley, A. Rushforth, M. Wang, G. Burnell, and T. Moore, Modification of perpendicular magnetic anisotropy and domain wall velocity in Pt/Co/Pt by voltage-induced strain, Sci. Rep. **5**, 7921 (2015).

[6] M. Farle, B. Mirwald-Schulz, A. Anisimov, W. Platow, and K. Baberschke, Higher-order magnetic anisotropies and the nature of the spin-reorientation transition in face-centered-tetragonal Ni(001)/Cu(001), Phys. Rev. B **55**, 3708 (1997).

[7] M. Johnson, P. Bloemen, F. Den Broeder, and J. De Vries, Magnetic anisotropy in metallic multilayers, Rep. Prog. Phys. **59**, 1409 (1996).

[8] Y. Millev and J. Kirschner, Reorientation transitions in ultrathin ferromagnetic films by thickness-and temperature-driven anisotropy flows, Phys. Rev. B **54**, 4137 (1996).

[9] P. Sharma, H. Kimura, A. Inoue, E. Arenholz, and J.-H. Guo, Temperature and thickness driven spin-reorientation

transition in amorphous Co-Fe-Ta-B thin films, Phys. Rev. B **73**, 052401 (2006).

[10] Q. Yang *et al.*, Spin-orbital coupling induced four-fold anisotropy distribution during spin reorientation in ultrathin Co/Pt multilayers, Appl. Phys. Lett. **110**, 022403 (2017).

[11] N. Nakajima, T. Koide, T. Shidara, H. Miyauchi, H. Fukutani, A. Fujimori, K. Iio, T. Katayama, M. Nyvlt, and Y. Suzuki, Perpendicular Magnetic Anisotropy Caused by Interfacial Hybridization via Enhanced Orbital Moment in Co/Pt Multilayers: Magnetic Circular X-Ray Dichroism Study, Phys. Rev. Lett. **81**, 5229 (1998).

[12] K. Kyuno, J. G. Ha, R. Yamamoto, and S. Asano, Theoretical study on the strain dependence of the magnetic anisotropy of X/Co ($X = \mathrm{Pt}$, Cu, Ag, and Au) metallic multilayers, J. Appl. Phys. **79**, 7084 (1996).

[13] J.-M. Hu, T. Yang, J. Wang, H. Huang, J. Zhang, L.-Q. Chen, and C.-W. Nan, Purely electric-field-driven perpendicular magnetization reversal, Nano Lett. **15**, 616 (2015).

[14] N. Pertsev, Giant magnetoelectric effect via strain-induced spin reorientation transitions in ferromagnetic films, Phys. Rev. B **78**, 212102 (2008).

[15] M. Liu, O. Obi, Z. Cai, J. Lou, G. Yang, K. S. Ziemer, and N. X. Sun, Electrical tuning of magnetism in Fe_3O_4/PZN-PT multiferroic heterostructures derived by reactive magnetron sputtering, J. Appl. Phys. **107**, 073916 (2010).

[16] M. Liu *et al.*, Electrically controlled non-volatile switching of magnetism in multiferroic heterostructures via engineered ferroelastic domain states, NPG Asia Mater. **8**, e316 (2016).

[17] O. Rousseau, R. Weil, S. Rohart, and A. Mougin, Strain-induced magnetic domain wall control by voltage in hybrid piezoelectric $BaTiO_3$ ferrimagnetic TbFe structures, Sci. Rep. **6**, 23038 (2016).

[18] J.-M. Hu, C.-W. Nan, and L.-Q. Chen, Size-dependent electric voltage controlled magnetic anisotropy in multiferroic heterostructures: Interface-charge and strain comediated magnetoelectric coupling, Phys. Rev. B **83**, 134408 (2011).

[19] Y. Chen, J. Wang, M. Liu, J. Lou, N. X. Sun, C. Vittoria, and V. G. Harris, Giant magnetoelectric coupling and *E*-field tunability in a laminated Ni_2MnGa/lead-magnesium-niobate-lead titanate multiferroic heterostructure, Appl. Phys. Lett. **93**, 112502 (2008).

[20] B. Guiffard, L. Seveyrat, G. Sebald, and D. Guyomar, Enhanced electric field-induced strain in non-percolative carbon nanopowder/polyurethane composites, J. Phys. D **39**, 3053 (2006).

[21] M. Liu, Z. Zhou, T. Nan, B. M. Howe, G. J. Brown, and N. X. Sun, Voltage tuning of ferromagnetic resonance with bistable magnetization switching in energy-efficient magnetoelectric composites, Adv. Mater. **25**, 1435 (2013).

[22] Y. Wang, S. W. Or, H. L. W. Chan, X. Zhao, and H. Luo, Enhanced magnetoelectric effect in longitudinal-transverse mode Terfenol-D/$Pb(Mg_{1/3}Nb_{2/3})O_3$-$PbTiO_3$ laminate composites with optimal crystal cut, J. Appl. Phys. **103**, 124511 (2008).

[23] M. Liu *et al.*, Giant electric field tuning of magnetic properties in multiferroic ferrite/ferroelectric heterostructures, Adv. Funct. Mater. **19**, 1826 (2009).

[24] G. Yu *et al.*, Strain-induced modulation of perpendicular magnetic anisotropy in Ta/CoFeB/MgO structures investigated by ferromagnetic resonance, Appl. Phys. Lett. **106**, 072402 (2015).

[25] M. Liu and N. X. Sun, Voltage control of magnetism in multiferroic heterostructures, Phil. Trans. R. Soc. A **372**, 20120439 (2014).

[26] M. Liu, B. M. Howe, L. Grazulis, K. Mahalingam, T. Nan, N. X. Sun, and G. J. Brown, Voltage-impulse-induced non-volatile ferroelastic switching of ferromagnetic resonance for reconfigurable magnetoelectric microwave devices, Adv. Mater. **25**, 4886 (2013).

[27] X. Guo *et al.*, Electric field induced magnetic anisotropy transition from fourfold to twofold symmetry in (001) $0.68Pb(Mg_{1/3}Nb_{2/3})O_3$-$0.32PbTiO_3/Fe_{0.86}Si_{0.14}$ epitaxial heterostructures, Appl. Phys. Lett. **108**, 152401 (2016).

[28] S. Sahoo, S. Polisetty, C. G. Duan, S. Jaswal, E. Tsymbal, and C. Binek, Ferroelectric control of magnetism in $BaTiO_3$/Fe heterostructures, in APS Meeting Abstracts, p. 32009 (2008).

[29] J.-W. Lee, S.-C. Shin, and S.-K. Kim, Spin engineering of CoPd alloy films via the inverse piezoelectric effect, Appl. Phys. Lett. **82**, 2458 (2003).

[30] J.-H. Kim, K.-S. Ryu, J.-W. Jeong, and S.-C. Shin, Large converse magnetoelectric coupling effect at room temperature in CoPd/PMN-PT(001) heterostructure, Appl. Phys. Lett. **97**, 252508 (2010).

[31] N. Lei, S. Park, P. Lecoeur, D. Ravelosona, C. Chappert, O. Stelmakhovych, and V. Holý, Magnetization reversal assisted by the inverse piezoelectric effect in Co-Fe-B/ferroelectric multilayers, Phys. Rev. B **84**, 012404 (2011).

[32] B. Peng *et al.*, Deterministic switching of perpendicular magnetic anisotropy by voltage control of spin reorientation transition in $(Co/Pt)_3/Pb(Mg_{1/3}Nb_{2/3})O_3$-$PbTiO_3$ multiferroic heterostructures, ACS Nano **11**, 4337 (2017).

[33] Y. Sun *et al.*, Electric-field modulation of interface magnetic anisotropy and spin reorientation transition in $(Co/Pt)_3$/PMN-PT heterostructure, ACS Appl. Mater. Interfaces **9**, 10855 (2017).

[34] G. Bochi, O. Song, and R. O'Handley, Surface magnetoelastic coupling coefficients of single-crystal fcc Co thin films, Phys. Rev. B **50**, 2043 (1994).

[35] E. Sabolsky, A. James, S. Kwon, S. Trolier-McKinstry, and G. Messing, Piezoelectric properties of ⟨001⟩ textured $Pb(Mg_{1/3}Nb_{2/3})O_3$-$PbTiO_3$ ceramics, Appl. Phys. Lett. **78**, 2551 (2001).

[36] S. Zhang *et al.*, Electric-Field Control of Nonvolatile Magnetization in $Co_{40}Fe_{40}B_{20}/Pb(Mg_{1/3}Nb_{2/3})_{0.7}Ti_{0.3}O_3$ Structure at Room Temperature, Phys. Rev. Lett. **108**, 137203 (2012).

[37] V. Grolier, J. Ferré, A. Maziewski, E. Stefanowicz, and D. Renard, Magneto-optical anisometry of ultrathin cobalt films, J. Appl. Phys. **73**, 5939 (1993).

[38] R. Desfeux, S. Bailleul, A. Da Costa, W. Prellier, and A. Haghiri-Gosnet, Substrate effect on the magnetic microstructure of $La_{0.7}Sr_{0.3}MnO_3$ thin films studied by magnetic force microscopy, Appl. Phys. Lett. **78**, 3681 (2001).

[39] C. Chappert, K. Le Dang, P. Beauvillain, H. Hurdequint, and D. Renard, Ferromagnetic resonance studies of very thin cobalt films on a gold substrate, Phys. Rev. B **34**, 3192 (1986).

[40] T. Li, S. Wu, A. Khan, A. M. Scotch, H. M. Chan, and M. P. Harmer, Heteroepitaxial growth of bulk single-crystal $Pb(Mg_{1/3}Nb_{2/3})O_3$–32 mol% $PbTiO_3$ from (111) $SrTiO_3$, J. Mater. Res. **14**, 3189 (1999).

[41] E. Liu *et al.*, Texture induced magnetic anisotropy in Fe_3O_4 films, Appl. Phys. Lett. **107**, 172403 (2015).

[42] C. Duran, S. Trolier-McKinstry, and G. L. Messing, Fabrication and electrical properties of textured $Sr_{0.53}Ba_{0.47}Nb_2O_6$ ceramics by templated grain growth, J. Am. Ceram. Soc. **83**, 2203 (2000).

[43] J. P. Remeika and W. M. Jackson, A method for growing barium titanate single crystals, J. Am. Chem. Soc. **76**, 940 (1954).

[44] T. Nan *et al.*, Quantification of strain and charge co-mediated magnetoelectric coupling on ultra-thin permalloy/PMN-PT interface, Sci. Rep. **4**, 3688 (2014).

[45] C.-G. Duan, J. P. Velev, R. F. Sabirianov, Z. Zhu, J. Chu, S. S. Jaswal, and E. Y. Tsymbal, Surface Magnetoelectric Effect in Ferromagnetic Metal Films, Phys. Rev. Lett. **101**, 137201 (2008).

[46] M. Liu, J. Hoffman, J. Wang, J. Zhang, B. Nelson-Cheeseman, and A. Bhattacharya, Non-volatile ferroelastic switching of the Verwey transition and resistivity of epitaxial Fe_3O_4/PMN-PT(011), Sci. Rep. **3**, 1876 (2013).

[47] Z. Wang, Y. Zhang, Y. Wang, Y. Li, H. Luo, J. Li, and D. Viehland, Magnetoelectric assisted 180 magnetization switching for electric field addressable writing in magnetoresistive random-access memory, ACS Nano **8**, 7793 (2014).